

TABLE V. Fit of  $\Delta V/V_0$  vs pressure.

Compound	$P$ (kbar)	$\Delta V/V_0$ (exp)	$(\Delta V/V_0)$ expt'l— $(\Delta V/V_0)$ calc
BeO	5	0.0019	0
	10	0.0037	0
	15	0.0052	0
	20	0.0065	0
	25	0.0076	0
	30	0.0086	0
	35	0.0093	0
	40	0.0097	0
	41	0.0098	0
	5	0.0115	0.0002
CdS	10	0.0200	0.0003
	15	0.0265	-0.0002
	20	0.0325	0
	23.4	0.0370	-0.0003
	30	0.2045	...
	35	0.2100	...
	40	0.2155	...
	43	0.2195	...
	5	0.0140	-0.0007
	10	0.0250	0.0003
CdSe	15	0.0340	0.0017
	20	0.0415	0.0020
	25.2	0.0480	-0.0013
	30	0.220	...
	35	0.227	...
	40	0.2340	...
	44	0.2385	...
	5	0.0175	-0.0002
	10	0.0315	-0.0004
	15	0.0435	0.0002
CdTe	20	0.0535	0.0007
	25	0.0620	0.0008
	30	0.0710	0.0013
	36	0.0805	0.0001
	40	0.2500	...
	43	0.2550	...
	5	0.0064	0
	10	0.0127	0.0000
	15	0.0188	0.0000
	20	0.0247	-0.0001
ZnS (sphalerite)	25	0.0303	0
	30	0.0358	0.0002
	35	0.0413	0.0005
	40	0.0464	0.0005
	42	0.0483	0.0005

used to calculate the shock Hugoniot locus for BeO of theoretical density. The pertinent equations are:

$$P_H - P_0 = (\gamma/V_H)(E_H - E_0), \quad (\text{Mie-Gruneisen})$$

where  $P_H$ ,  $E_H$ =pressure and specific internal energy

TABLE VI. Dynamic data for BeO.

Initial density $\rho_0$ (g/cm <sup>3</sup> )	Shock velocity $U_s$ (cm/ $\mu$ sec)	Particle velocity $U_p$ (cm/ $\mu$ sec)	$P$ (kbar)	$V/V_0$	
				Experi- mental	Normal- ized to theoretical density
2.908	0.865	0.78	197	0.912	0.942
2.905	0.929	1.25	338	0.866	0.895
2.909	0.962	1.56	437	0.838	0.866
2.919	1.015	1.91	566	0.812	0.839
2.914	1.022	2.06	613	0.798	0.824
2.910	1.085	2.42	765	0.777	0.803
2.926	1.126	2.74	905	0.765	0.782
2.914 (Av.)	0.760	0	0	1.000	1.033

TABLE VII. Assumed constants for BeO.

$\gamma_0$	$C_V$ (cal/mole °K)	$(\partial P/\partial T)_V$ (bar/°K)	$E_1$ (cal/mole)
1.97	2.91	28	690

along the Hugoniot and  $P_0$ ,  $E_0$ =pressure and specific internal energy along a reference curve.

$$E_H - E_1 = \frac{1}{2} P_H (V_1 - V_H), \quad (\text{Hugoniot})$$

where  $E_1$ ,  $V_1$ =specific internal energy and volume at  $P=0$ . Here  $V_1=1/\rho_0$ , where  $\rho_0$  is the theoretical density.

In this case the reference curve employed was the experimental Hugoniot curve (see Table VIII).

The final equation in terms of  $P_H$  and  $V_H$  is

$$P_H = \frac{(E_1 - E_0) + (V_H/\gamma)P_0}{V_H/\gamma - (1/2)(V_1 - V_H)}.$$

Therefore the Hugoniot for theoretical density was calculated and the temperatures along the Hugoniot were also determined.<sup>11</sup> The corresponding 25°C isotherm was calculated by assuming  $(\partial P/\partial T)_V$  was constant. Thus at constant volume, the pressure correction was

$$\Delta P = (\partial P/\partial T)_V \Delta T.$$

These results are shown in Table VIII and in Fig. 2.

In the codes used to calculate temperatures  $C_V$  is assumed constant. Unfortunately, the value for  $C_V$  is about one-half the Dulong and Petit limit. The maximum temperatures calculated along the Hugoniot are over 1000°C and at these temperatures  $C_V$  has probably reached the Dulong and Petit value. The effect of  $C_V$  increasing in this manner is that the calculated temperatures are too high, and the corresponding pressure corrections are too large. The true 25°C isotherm is then somewhere between the two dotted curves in Fig. 2. However, the error is negligible at lower pressure and the comparison between the hydrostatic data and the 25°C isotherms should be valid. However, the data are

TABLE VIII. Calculated Hugoniot and 25°C isotherm. BeO at theoretical density.

$V/V_0$	Hugoniot		25°C isotherm
	$P$ (kbar)	$T$ (°C)	$P$ (kbar)
1.000	0	25	0
0.980	40	33	40
0.96	83	46	83
0.94	129	69	128
0.92	184	105	182
0.90	244	156	240
0.88	311	240	305
0.86	388	359	379
0.84	474	544	460
0.82	569	776	548
0.80	678	1110	648
0.78	800	1512	758



in poor agreement. This is probably due to the scatter in the hydrostatic data. Thus, we believe the Hugoniot measurements to be superior to the hydrostatic work in this case.

The phase transformation predicted by Jaryaraman *et al.*<sup>3</sup> for BeO was not observed.

### ZnO

The ZnO was in the form of a small crystal about 0.0625 in. in diameter by 1 in. long. The sample was too small for the 0.5-in. die so that a 0.132-in.-diam die was used. The measured isothermal compressibility is listed in Table III, but the adiabatic compressibility calculated from the elastic constants is considered more reliable. This is mainly due to the large friction corrections associated with compression of the small crystal.

The ZnO did not convert to the sphalerite under these conditions. This was verified by x-ray studies after pressurization.

### ZnS

The ZnS samples were obtained from a number of sources of which Harshaw provided the only hexagonal crystals. This fact was relatively unimportant because the hexagonal form always converted to the sphalerite form under pressure. This fact, combined with knowledge of the scarcity of hexagonal crystals in nature, as well as the problem in growing a wurtzite crystal, lead us to the conclusion that the wurtzite form of ZnS is metastable under normal conditions. The data on compressibility in Fig. 3 are therefore compared with Bridgman's<sup>20</sup> data; it may be seen that the agreement is good. The agreement between the adiabatic and isothermal compressibilities is also good.

### CdS

The CdS samples were obtained from various sources and were all essentially equivalent. The compressibility data are plotted in Fig. 4. The solid-state transformation to the rocksalt form has been identified by others using x-ray techniques.<sup>4-6</sup> We believe that the transformation pressures obtained in this work are quite accurate.

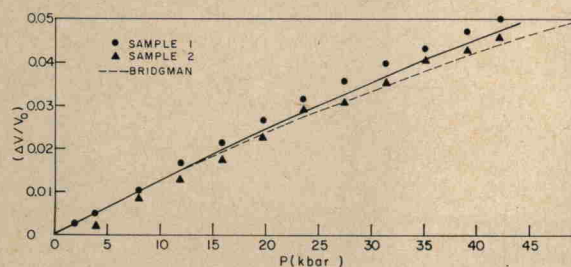


FIG. 3. Compression of ZnS, sphalerite structure.

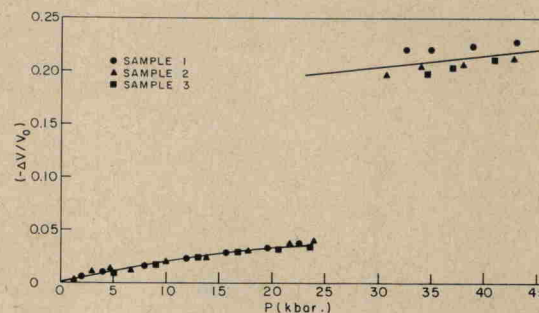


FIG. 4. Compression of CdS.

There is hysteresis in the transition on the increasing and decreasing pressure cycles; the pressures were averaged in Table IX. These data are compared with the data of Jayaraman<sup>3</sup> and others in Table X. Table XI

TABLE IX. Transformation pressures in II-VI Cd compounds.

Compound	Transformation pressure (kbar)	
CdSe	Increased pressure	25.2±1
	Decreased pressure	17.2±0.7
	Average pressure	21.3±0.8
CdS	Increased pressure	23.4±0.6
	Decreased pressure	11.4±1.0
	Average pressure	17.5±0.8
CdTe	Increased pressure	34.9±0.2
	Decreased pressure	28.6±0.8
	Average pressure	31.8±0.5

tabulates the volume changes observed in this work and that of previous investigators.

The compressed CdS samples returned to 1 atm pressure as a mixture of the sphalerite and wurtzite forms, with the sphalerite form predominant. This is consistent with the reverse structural sequence<sup>5</sup> rocksalt → sphalerite → wurtzite. The agreement between the adiabatic and isothermal compressibility is poor (see Table III).

TABLE X. Transformation pressures in II-VI Cd compounds.

Compound	Investigator	$P_T$ (kbar)
CdS	Cline and Stephens	17.5±0.8
	Jayaraman <i>et al.</i>	20
	Mariano and Warekois	33 <sup>a</sup>
	Rooymans	20 <sup>a</sup>
	Samara and Drickamer	~20-30
	Edwards <i>et al.</i>	27.5
CdSe	Cline and Stephens	21.3±0.8
	Jayaraman <i>et al.</i>	~19
	Mariano and Warekois	32 <sup>a</sup>
	Rooymans	30 <sup>a</sup>
CdTe	Cline and Stephens	31.8±0.5
	Jayaraman <i>et al.</i>	33
	Mariano and Warekois	36 <sup>a</sup>
	Samara and Drickamer	30-35

<sup>a</sup> Pressure applied is not necessarily the transformation pressure.

<sup>20</sup> P. W. Bridgman, Am. Acad. Arts Sci. 74, 21 (1940).